

PATHWAYS TO OXYGEN-BEARING MOLECULES IN THE INTERSTELLAR MEDIUM AND IN PLANETARY ATMOSPHERES: CYCLOPROPENONE (c-C₃H₂O) AND PROPYNAL (HCCCHO)

LI ZHOU AND RALF I. KAISER

Department of Chemistry, University of Hawaii at Manoa, Honolulu, HI; ralfk@hawaii.edu

LI GYUN GAO AND AGNES H. H. CHANG¹
National Dong Hwa University, Hualien, 974, Taiwan

MAO-CHANG LIANG

Research Center for Environmental Changes, Academia Sinica, Taipei, Taiwan

AND

YUK L. YUNG

Division of Geological and Planetary Sciences, Caltech, Pasadena, CA

Received 2008 February 20; accepted 2008 June 10

ABSTRACT

We investigated the formation of two C₃H₂O isomers, i.e., cyclopropenone (c-C₃H₂O) and propynal (HCCCHO), in binary ice mixtures of carbon monoxide (CO) and acetylene (C₂H₂) at 10 K in an ultrahigh vacuum machine on high-energy electron irradiation. The chemical evolution of the ice samples was followed online and in situ via a Fourier transform infrared spectrometer and a quadrupole mass spectrometer. The temporal profiles of the cyclopropenone and propynal isomers suggest (pseudo-) first-order kinetics. The cyclic structure (c-C₃H₂O) is formed via an addition of triplet carbon monoxide to ground-state acetylene (or vice versa); propynal (HCCCHO) can be synthesized from a carbon monoxide–acetylene complex via a [HCO...CCH] radical pair inside the matrix cage. These laboratory studies showed for the first time that both C₃H₂O isomers can be formed in low-temperature ices via nonequilibrium chemistry initiated by energetic electrons as formed in the track of Galactic cosmic ray particles penetrating interstellar icy grains in cold molecular clouds. Our results can explain the hitherto unresolved gas phase abundances of cyclopropenone in star-forming regions via sublimation of c-C₃H₂O as formed on icy grains in the cold molecular cloud stage. Implications for the heterogeneous oxygen chemistry of Titan and icy terrestrial planets and satellites suggest that the production of oxygen-bearing molecules such as C₃H₂O may dominate on aerosol particles compared to pure gas phase chemistry.

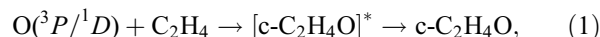
Subject headings: astrobiology — astrochemistry — ISM: molecules — planets and satellites: individual (Titan)

Online material: color figures

1. INTRODUCTION

The detection of carbon monoxide (CO) in the atmospheres of Jupiter (Beer 1975), Saturn (Noll et al. 1986), Uranus (Rosenqvist et al. 1992), Neptune (Rosenqvist et al. 1992; Courtin et al. 1996), and Pluto (Bockelee-Morvan et al. 2001) at mixing ratios of about 10⁻⁹, (2.0 ± 0.7) × 10⁻⁹ to (3 ± 1) × 10⁻⁷, 4 × 10⁻⁸, (6.5 ± 3.5) × 10⁻⁷ to (2.7 ± 1.8) × 10⁻⁶, and 7 × 10⁻² to 10⁻¹, respectively, suggests that a coupling between the hydrocarbon and oxygen chemistry might exist in hydrocarbon-rich atmospheres of planets and their moons (Bernard et al. 2003). Carbon monoxide was also identified in Titan's atmosphere at the 60 ppm level in the *Voyager* time and at the 32 ± 15 ppm level recently based on the *Cassini* VIMS spectral imaging (Baines et al. 2006); carbon dioxide (CO₂) was suggested to hold fractional abundances in the range of 16 ± 2 ppb (de Kok et al. 2007), several orders of magnitude less than carbon monoxide. The hypothesis of a coupled oxygen–hydrocarbon chemistry gained support from the latest laboratory experiments. These studies simulated the chemical processing of Titan's atmosphere in the bulk and indicated that the incorporation of carbon monoxide into Titan's gas phase and aerosol chemistry could lead to oxygen-bearing compounds, among them ethylene oxide (oxirane; c-C₂H₄O) as dominant

species (Bernard et al. 2003) (Fig. 1). This molecule can be formed by reactions of suprathreshold, ground, and/or electronically excited oxygen atoms with ethylene (C₂H₄) followed by a stabilization of the rovibrationally excited intermediate via a third-body collision combined with intersystem crossing (Bennett et al. 2005a) (eq. [1]). Note that oxirane has also been detected in star-forming regions such as Sgr B2 (Guzmán et al. 1997; Nummelin et al. 1998), a region where molecules formed on icy grains in the cold molecular cloud stage can sublime into the gas phase. Therefore, it is intriguing to investigate whether a common synthetic route to oxygen-carrying molecules could exist in extreme environments. However, only limited laboratory studies have been conducted so far on the formation of oxygen-bearing molecules in the interstellar medium and in hydrocarbon-rich atmospheres of planets and their moons. These investigations have been limited to the synthesis of oxirane (c-C₂H₄O) from oxygen atoms and ethylene as discussed above (eq. [1]) (Bennett et al. 2005a), and of its acetaldehyde isomer (CH₃CHO) formed in carbon monoxide–methane ices (Bennett et al. 2005b) via reaction (2) through a [CH₃-HCO] radical pair,



In this paper, we expand the previous investigations and present a combined experimental, theoretical, and modeling study on

¹ Current address: Graduate Institute of Astronomy, National Central University, Zhongli, Taiwan.

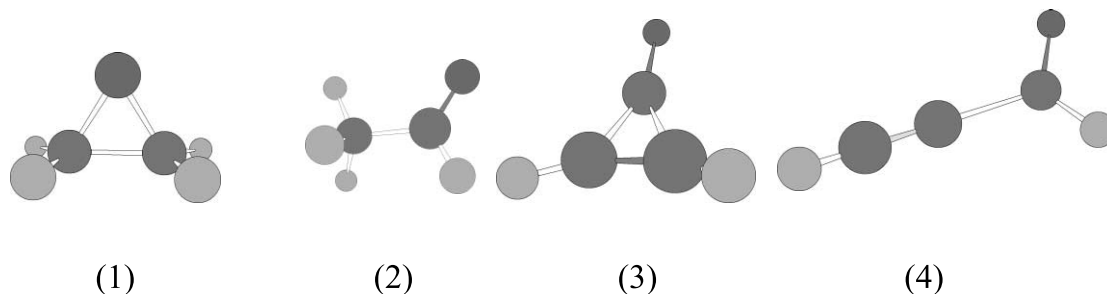
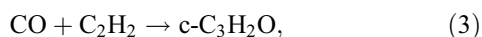


FIG. 1.—Three-dimensional structures of oxygen-bearing molecules: oxirane (1), acetaldehyde (2), cyclopropanone (3), and propynal (4). [See the electronic edition of the Journal for a color version of this figure.]

the formation routes to the oxygen-bearing molecules of the generic formula C_3H_2O in extreme environments. We focus on the structural isomers cyclopropanone ($c\text{-}C_3H_2O$) and propynal (HCCCHO; Fig. 1), which in principle can be synthesized via nonequilibrium reactions of carbon monoxide (CO) with acetylene (C_2H_2) on interstellar grains and aerosol particles in hydrocarbon-rich atmospheres (reactions [3] and [4]). Recall that both C_3H_2O molecules have been detected in the interstellar medium. Propynal was first observed in 1988 toward the cold molecular cloud TMC-1 with fractional abundances of about $(1.5 \pm 0.4) \times 10^{-10}$ (Irvine et al. 1988). A subsequent search in the hot core of Sagittarius B2 yielded only upper limits (Turner 1991). On the other hand, the cyclic isomer, cyclopropanone, is absent in cold molecular clouds, but has been detected recently toward Sagittarius B2 with fractional abundances of about 6×10^{-11} (Hollis et al. 2006). Therefore, our investigation can shed light on the production routes of both isomers in interstellar environments and also on the potential role of the C_3H_2O family as possible oxygen-bearing precursors to be incorporated into the organic haze layers of Saturn's moon Titan. For simplicity, we conduct the simulation experiments at 10 K first. In previous studies on the related $C_2H_4O_2$ (Bennett et al. 2005b) and C_2H_4O systems (Bennett et al. 2007), this helped to elucidate basic reaction mechanisms and to discriminate between thermal and nonthermal pathways leading to distinct isomers. The simulation temperature directly mimics the conditions of icy, interstellar grains as present in cold molecular clouds such as in TMC-1, which are exposed to high-energy Galactic cosmic ray particles. On penetrating the ices, the latter divert their energy almost exclusively via electronic interaction with the target molecules (Kaiser & Roessler 1997) leading to the generation of cascades of secondary electrons. Galactic cosmic ray particles (GCRs) consist of about 98% protons (p , H^+) and 2% helium nuclei (α -particles, He^{2+}). It has been shown that, for example, a 10 MeV proton transfers 99.99% of the energy into the ice target to the electronic system of the target molecules via a linear energy transfer (LET) of a few $keV \mu m^{-1}$; a similar LET is found for 5 keV electrons as they penetrate ices (for more detailed discussions on the effects of irradiation on ices, please refer to (Kaiser 2002; Bennett et al. 2005b)). Therefore, to mimic the formation of C_3H_2O isomers within interstellar ices, we chose to investigate the effects of 5 keV electrons, which have a similar linear energy transfer compared to the MeV protons (see § 2), on binary ice mixtures of carbon monoxide and acetylene. Implications for the chemical processing of hydrocarbon-rich atmospheres of planets and their satellites are also given,



2. EXPERIMENTAL

The simulation experiments were conducted in an ultrahigh vacuum chamber operated at base pressures of about 3×10^{-11} torr. Briefly, the main chamber consists of a 15 l cylindrical stainless steel chamber of 250 mm diameter and 300 mm height which is evacuated by a magnetically suspended turbo pump backed by an oil-free scroll pump (Bennett et al. 2004). A two-stage closed cycle helium refrigerator—interfaced to a differentially pumped rotary feedthrough—is attached to the lid of the machine and holds a polished silver single crystal. This crystal is cooled to 10.4 ± 0.3 K, serves as a substrate for the ice condensate, and conducts the heat generated from the impinging electrons to the cold head. The ice condensation is assisted by a precision leak valve. The carbon monoxide ($^{12}C^{16}O$)–acetylene ($^{12}C_2H_2$) ices were prepared at 10.4 K by depositing premixed gases (60 torr CO 99.99%, the Specialty Gas Group; 64 torr C_2H_2 99.99%, the Specialty Gas Group) at pressures of 10^{-8} torr for 10 minutes. Acetone traces in the acetylene gas were removed by a zeolite trap and an acetone-dry ice bath. To determine the ice composition quantitatively, we integrated the ν_1 (2141 cm^{-1} ; Jiang et al. 1975b) and ν_2 (1960 cm^{-1} ; Nakayama & Watanabe 1964) absorption features of carbon monoxide and acetylene, respectively, and calculated the thicknesses of the carbon monoxide–acetylene ices to be 97 ± 9 nm using densities of carbon monoxide and acetylene of 1.03 g cm^{-3} (CO ice; 10 K; Jiang et al. 1975a) and 0.76 g cm^{-3} (Tarasova 1982). The carbon monoxide to acetylene ratio was determined to be about 1.0 ± 0.1 . Control experiments were also conducted with $^{12}C^{18}O\text{-}^{12}C_2H_2$ and $^{12}C^{16}O\text{-}^{12}C_2D_2$ ices to confirm the mass spectrometric and infrared spectrometric assignments.

All ices were irradiated isothermally at 10.4 K with 5 keV electrons generated in an electron gun (Specs EQ-22/35) at beam currents of 100 nA (60 minutes) by scanning the electron beam over an area of $3.0 \pm 0.4 \text{ cm}^2$. It should be stressed that control experiments with pure carbon monoxide samples and of pure acetylene samples did not show any evidence of stable ions formed. Accounting for irradiation times and the extraction efficiency of 78.8% of the generated electrons, this exposes the target to 1.8×10^{15} electrons. The electron trajectories were simulated using the CASINO code (Drouin et al. 2001). The results indicate that average energy of electrons after they have been transmitted through the sample is 4.61 ± 0.04 keV. This means that each electron transfers on average a total of 390 ± 40 eV per electron into the sample. This value corresponds to an average LET of $3.9 \pm 0.4 \text{ keV } \mu m^{-1}$, and therefore exposing our sample to an average dose of 1.2 ± 0.2 eV per molecule. After the irradiation, the sample was kept isothermal at 10.4 K for 60 minutes and heated then by $0.5 \text{ K minute}^{-1}$ to 300 K. The infrared spectra of the samples were measured *online* and *in situ* by a Fourier

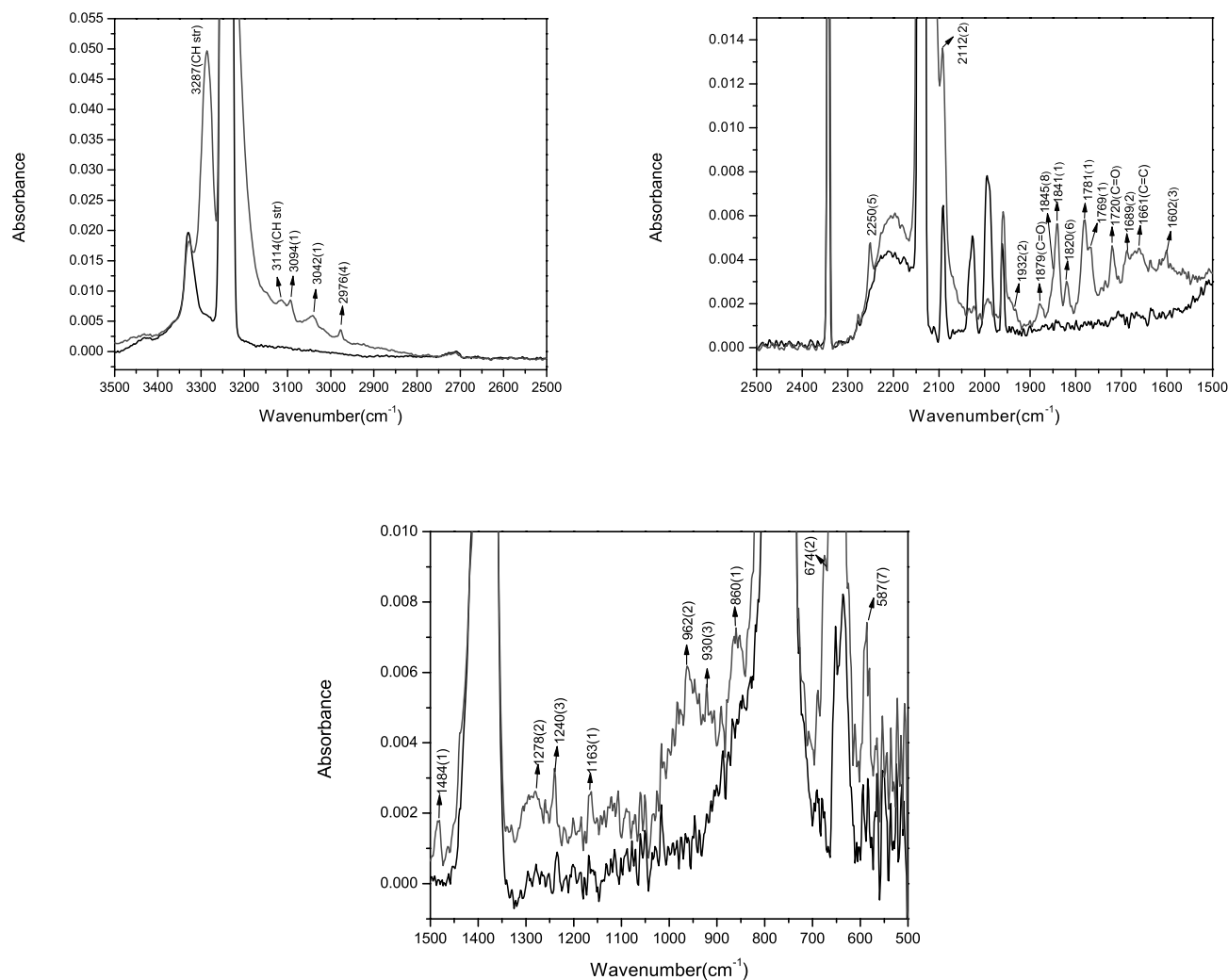


FIG. 2.—Infrared spectra taken before (*black lines*) and after (*gray lines*) the irradiation of the carbon monoxide-acetylene ice at 10.4 K: (1) cyclopropenone, (2) propynal, (3) vinylacetylene, (4) H_2CCCO , (5) C_3O , (6) C_5O , (7) C_3O_2 , (8) HCO. [See the electronic edition of the *Journal* for a color version of this figure.]

transform infrared spectrometer (Nicolet 6700 FTIR) from the irradiation to the heating phase (Bennett et al. 2004). We also utilized a quadrupole mass spectrometer (Balzer QMG 420) to monitor the species released into the gas phase (mass range: 1–200 amu) via electron impact ionization of the neutral molecules with 90 eV electrons.

3. THEORY

3.1. Computations

Ab initio electronic structure calculations are performed for the reaction of acetylene with carbon monoxide for probable channels on both adiabatic triplet and singlet ground-state potential energy surfaces of $\text{C}_3\text{H}_2\text{O}$. The collision complexes and their subsequent isomerization pathway via ring opening, ring formation, and hydrogen migration are sought out. The collision complexes, intermediates, and transition states are characterized such that the optimized geometries, harmonic frequencies, and the energies with zero-point energy corrections are obtained. The ab initio calculations are carried out at the level of the hybrid density functional theory, the unrestricted B3LYP (Lee et al. 1988; Becke 1993)/6–311 G(d, p) (McLean & Chandler 1980; Krishnan et al. 1980), by utilizing the GAUSSIAN 98 programs (Frisch et al. 2001). The energies are further refined with the coupled cluster

CCSD(T) (Purvis & Bartlett 1982; Raghavachari et al. 1989)/cc-pVTZ (Dunning 1989) with B3LYP/6–311G(d, p) zero-point energy corrections at their B3LYP/6–311G(d, p) optimized geometries.

3.2. Modeling

To evaluate the production of oxygen compounds via heterogeneous processes in planetary conditions, we select Titan as an example for a detailed study. A one-dimensional photochemical model is used. The aforementioned yields of oxygen compounds are incorporated into an existing model described elsewhere (Liang et al. 2007). The model chemistry is based on Moses et al. (2005), which contains the most updated hydrocarbon and oxygen chemistry, along with physiochemical processes. We select Model D of Liang et al. (2007) as a reference case for the study. The proposed formation routes of the oxygen compounds require high-energy cosmic rays; the energy deposition was estimated to be $10^9 \text{ eV cm}^{-2} \text{ s}^{-1}$ from Sagan & Thompson (1984).

4. RESULTS

4.1. Infrared Spectroscopy

The analysis of the infrared spectra is carried out in three steps. First, we investigate the appearance of new absorptions qualitatively and assign their carriers. Hereafter, the temporal

TABLE 1
NEW ABSORPTION FEATURES IN THE IRRADIATED ACETYLENE-CARBON MONOXIDE SAMPLES

Absorption	Literature	Assignment	Carrier
3287.....	CH stretch in $-C \equiv C-H$
3114.....	CH stretch in $RCH = CH_2$
3094.....	3096	ν_1 C-H stretch	Cyclopropenone
3042.....	3062	ν_9 C-H stretch	Cyclopropenone
2976.....	2978	ν_{11} CH stretch (C_3H_2O)	OCCCH ₂
2250.....	2249	ν_1	C ₃ O
2112.....	2125	ν_3	Propynal
1932.....	1925	$2 \times \nu_{10}$	Propynal
1879.....	C = O in methyl ketones
1845.....	1845	C = O stretch	Formyl (HCO)
1841.....	1840	ν_2 C = O stretch	Cyclopropenone
1820.....	1817	ν_3	C ₃ O
1781.....	1792	$2 \times \nu_{11}$	Cyclopropenone
1769.....	1770	$2 \times \nu_{11}$	Cyclopropenone
1720.....	C = O in saturated ketones/aldehydes
1689.....	1692	ν_4	Propynal
1661.....	C = C stretch in isolated $-C = C-$
1602.....	1599	ν_6	Vinylacetylene
1484.....	1485	ν_3 C = C stretch	Cyclopropenone
1278.....	1275	$2 \times \nu_{11}$	Propynal
1240.....	1244	$2 \times \nu_{11}$	Vinylacetylene
1163.....	1160	ν_{10} C-C stretch	Cyclopropenone
962.....	950	ν_6	Propynal
930.....	927	ν_{15}	Vinylacetylene
674.....	669	ν_{11}	Propynal
587.....	577	ν_6	C ₃ O ₂

NOTE.—Spectra were recorded at 10.4 K after the radiation exposure.

developments of these absorptions on electron irradiation—by focusing on the molecules related to the formation of the C_3H_2O isomers—are investigated quantitatively. Finally, these data are fit to derive the reaction mechanism, the kinetics, and the production rates of newly synthesized C_3H_2O molecules.

The effects of the electron bombardment of the binary ice mixtures are compiled in Figure 2. A comparison of the non-irradiated sample (*black line*) with the exposed ice (*gray line*) at 10.4 K identifies various novel absorption features (Table 1). First, we can assign seven peaks to the cyclopropenone molecule ($c-C_3H_2O$). These are the ν_1 (3094 cm^{-1}), ν_9 (3042 cm^{-1}), ν_2 (1841 cm^{-1}), $2\nu_{11}$ ($1781, 1769\text{ cm}^{-1}$), ν_3 (1484 cm^{-1}), ν_{10} (1163 cm^{-1}), and ν_5 (860 cm^{-1}). The position of these absorptions agree very well with previous literature data of ν_1 (3096 cm^{-1}), ν_9 (3062 cm^{-1}), ν_2 (1840 cm^{-1}), $2\nu_{11}$ ($1792, 1770\text{ cm}^{-1}$), ν_3 (1485 cm^{-1}), ν_{10} (1160 cm^{-1}), and ν_5 (851 cm^{-1}) (Brown et al. 1975). The identification of this molecule has also been confirmed in the irradiated $^{12}C^{16}O-^{12}C_2D_2$ ices via the observation of five absorptions of D2-cyclopropenone: $\nu_3 + \nu_{12}$ (1878 cm^{-1} ; 1878 cm^{-1}), ν_2 (1788 cm^{-1} ; 1776 cm^{-1}), ν_3 (1411 cm^{-1} ; 1409 cm^{-1}), ν_{11} (782 cm^{-1} ; 791 cm^{-1}), and ν_7 (671 cm^{-1} ; 697 cm^{-1}); the values in italics indicate literature data taken from Brown et al. (1975) which agree very nicely with the observations. In the $^{12}C^{18}O-^{12}C_2H_2$ system, we were also able to observe the ν_{10} mode at 1850 cm^{-1} (1861 cm^{-1}).

Second, the infrared spectra showed six absorptions which can be attributed to the propynal isomer (HCCCHO). These are: ν_3 (2112 cm^{-1} ; 2125 cm^{-1}), $2\nu_{10}$ (1932 cm^{-1} ; 1925 cm^{-1} ; shoulder), ν_4 (1689 cm^{-1} ; 1692 cm^{-1}), $2\nu_{11}$ (1278 cm^{-1} ; 1275 cm^{-1}), ν_6 (962 cm^{-1} ; 950 cm^{-1}), and ν_{11} (674 cm^{-1} ; 669 cm^{-1} ; shoulder; King & Moule 1961). Similar to the D2-cyclopropenone, we were also able to confirm the identification of the propynal species by detecting its D2-isotopologue in the irradiated

$^{12}C^{16}O-^{12}C_2D_2$ samples via the ν_{11} (2114 cm^{-1} ; 2124 cm^{-1}), ν_9 (1710 cm^{-1} ; 1709 cm^{-1}), and ν_7 (869 cm^{-1} ; 861 cm^{-1}) absorptions. Likewise, the $^{12}C^{18}O-^{12}C_2H_2$ ices depict novel absorptions at 1676 cm^{-1} (ν_9 ; 1673 cm^{-1}), 919 cm^{-1} (ν_6 ; 923 cm^{-1}), and 665 cm^{-1} (ν_4 ; 665 cm^{-1}). We would like to stress that a third isomer, propadienone (H_2CCCO) could be assigned only *tentatively* via a single absorption at 2976 cm^{-1} (ν_{11} ; 2978 cm^{-1} ; Chapman et al. 1987).

Besides the C_3H_2O isomers, we found several additional molecules in the irradiated samples. These could be assigned to the formyl radical (HCO; 1845 cm^{-1} , 1845 cm^{-1} , ν_1), vinylacetylene ($HCCCH_2$; 1602 cm^{-1} , 1599 cm^{-1} , ν_6 ; 1240 cm^{-1} , 1244 cm^{-1} , $2\nu_{11}$; 930 cm^{-1} , 927 cm^{-1} , ν_{15} ; Tørnøng et al. 1980), and tentatively to C_3O (2250 cm^{-1} , 2249 cm^{-1} , ν_1), C_3O (1820 cm^{-1} , 1817 cm^{-1} , ν_3), and C_3O_2 (587 cm^{-1} , 577 cm^{-1} , ν_6). The last three molecules could be also detected in electron-irradiated pure carbon monoxide samples at 10 K studied previously in our laboratory (Jamieson et al. 2006). Finally, the irradiated samples depicted absorption features which could not be assigned to individual molecular carriers, but only to functional groups as compiled in Table 1.

4.2. Mass Spectrometry

We are now comparing the infrared observations with a mass spectrometric analysis of the gas phase. During the irradiation and isothermal phases, no molecules were observed to be released into the gas phase. However, when the temperature is increased, we monitor a sublimation of the carbon monoxide ($m/z = 28$) and acetylene ($m/z = 26$) matrix with an onset of about 60 K. Blank checks, i.e., experiments carried out under identical conditions, but *without* an electron irradiation of the ices, showed no additional molecules released into the gas phase. However, on warming up the irradiated sample to 300 K, signal

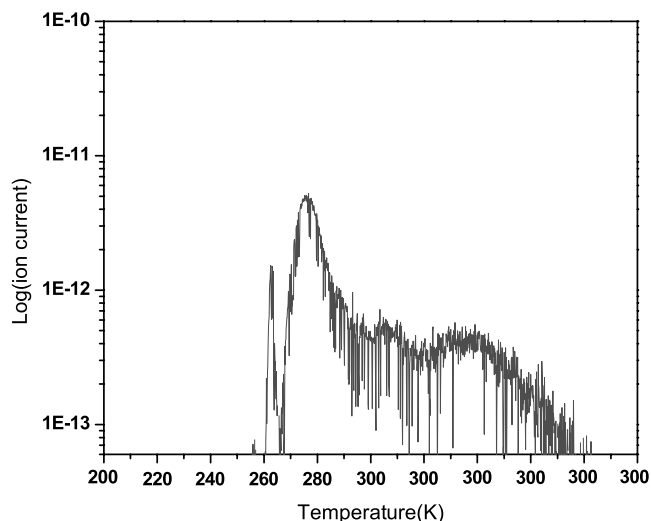
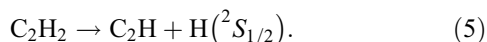


FIG. 3.— Evolution of the ion counts at mass to charge of $m/z = 54(\text{C}_3\text{H}_2\text{O}^+)$ in the warming-up phase. The target was warmed up from 10 to 300 K at a rate of $0.5 \text{ K minute}^{-1}$ and then kept isothermally at 300 K. [See the electronic edition of the Journal for a color version of this figure.]

appeared at $m/z = 54 (\text{C}_3\text{H}_2\text{O}^+)$; Fig. 3). Signal at higher mass-to-charge ratios was not detected. It should be noted that we also observed signal at $m/z = 52$. This could come from dissociative ionization of the neutral $\text{C}_3\text{H}_2\text{O}$ molecules in the electron impact ionizer and/or from the parent ion of vinylacetylene (C_4H_4^+), which was identified via infrared spectroscopy (§ 4.1). We should remind the reader that based on the mass spectrometric data alone, we cannot quantify to what extent signal at $m/z = 54$ originates from cyclopropenone and/or propynal. However, the infrared data help to elucidate the formation rates quantitatively. To verify the assignment of the $\text{C}_3\text{H}_2\text{O}^+$ molecular ions, we also conducted experiments with $^{12}\text{C}^{18}\text{O}-^{12}\text{C}_2\text{H}_2$. Here, signal was observed at $m/z = 56 (^{12}\text{C}_3\text{H}_2^{18}\text{O}^+)$, thus verifying the observations conducted in the $^{12}\text{C}^{16}\text{O}-^{12}\text{C}_2\text{H}_2$ system. Summarized, the most important information from the mass spectra are the verification of the formation of $\text{C}_3\text{H}_2\text{O}$ and the absence of molecular hydrogen released into the gas phase.

5. DISCUSSION

Having identified the cyclopropenone ($c\text{-C}_3\text{H}_2\text{O}$) and propynal (HCCCHO) molecules in electron-irradiated acetylene-carbon monoxide ices at 10.4 K, we would now like to kinetically fit the temporal evolution of the profiles of both isomers and of the formyl (HCO) radical during the irradiation of our sample (Fig. 4). Our results suggest that the initial step in the formation of propynal (HCCCHO) is the electron-induced unimolecular decomposition of the acetylene molecule via cleavage of a carbon-hydrogen bond to generate an ethynyl radical and a hydrogen atom (reaction [5]),

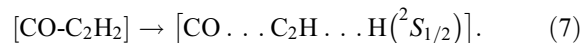


This reaction is endoergic and requires by 468 kJ mol^{-1} (4.9 eV). The CASINO calculations (§ 2) showed that one electron releases $390 \pm 40 \text{ eV}$ to the sample molecules on average. The hydrogen atom holds an excess energy of a few electron volts (Bennett et al. 2005b); this suprathreshold hydrogen atom can pass the barrier of addition and, hence, can add to the carbon-oxygen double bond of the carbon monoxide molecule, forming a formyl radical (eq. [6]). Keller et al. (1996), Woon (1996), and Jursic (1998) studied the system $\text{H}(^2\text{S}_{1/2}) + \text{CO}(X^1\Sigma^+) \rightarrow \text{HCO}(X^2A')$ extensively and reported that the best theoretical values of the entrance barrier

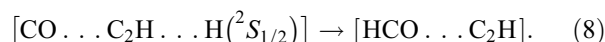
and the reaction energy are 10.5 and $-59.8 \text{ kJ mol}^{-1}$, respectively. The corresponding experimental values are 8.3 ± 1.7 (Wang et al. 1973) and $-58.6 \text{ kJ mol}^{-1}$ (Werner et al. 1995), respectively;



What is the fate of the HCO radicals? If the carbon monoxide is neighboring an acetylene molecule, i.e., represented *formally* as a $[\text{CO}-\text{C}_2\text{H}_2]$ complex in the solid ice, the carbon-hydrogen bond cleavage releases a hydrogen atom to form an ethynyl radical and a hydrogen atom in the *matrix cage*:



Due to energy and momentum conservation, the hydrogen atom holds an excess kinetic energy (suprathreshold hydrogen atoms) which can be either utilized to escape from the matrix cage or to overcome the barrier to add to the carbon monoxide molecule forming the formyl radical *within* the matrix cage,



This mechanism would be first order with respect to the appearances of the ethynyl and the formyl radicals, respectively. If the formyl and ethynyl radicals have the correct geometrical orientation, they can recombine within the matrix cage to form the propynal molecule without barrier (eq. [9]). However, if the geometry does not allow a barrier-less recombination reaction, both the formyl and the ethynyl radical should be observable spectroscopically,



Based on these considerations, we utilize equations (10) and (11) to fit the temporal profile of the formyl radical and of the propynal molecules via pseudo-first order reaction formally via a unimolecular decomposition of a $[\text{CO}-\text{C}_2\text{H}_2]$ complex in the irradiated ices (Bennett et al. 2005b). This reaction sequence is similar to the one observed in the formation of acetaldehyde (CH_3CHO) in methane-carbon monoxide ices via reaction (2) (Bennett et al. 2005b). This procedure yields rate constants of $k_1 = (7.4 \pm 2.5) \times 10^{-2} \text{ s}^{-1}$ and $k_2 = (9.0 \pm 0.6) \times 10^{-2} \text{ s}^{-1}$ as well as a and b values of 0.75 ± 0.25 and 2.37 ± 0.5 , respectively. Both rate constants are in the same order of magnitude. It should be stressed that the ethynyl radical remains unobservable in the matrix since its ν_1 and ν_3 fundamentals of 3298 cm^{-1} and $1835\text{--}1846 \text{ cm}^{-1}$ (Stephens et al. 1988; Forney et al. 1995) overlap with the absorptions of the acetylene molecules (Bell & Nielsen 1950). Likewise, we were able to fit the temporal profile of the cyclopropenone ($c\text{-C}_3\text{H}_2\text{O}$) isomer with first order kinetics via equation (12) ($c = 1.1 \pm 0.2$; $k_3 = (2.8 \pm 0.4) \times 10^{-2} \text{ s}^{-1}$). This may imply that neighboring carbon monoxide-acetylene molecules can also react in a (pseudo-) one step reaction to form cyclopropenone of the appropriate geometrical orientation. A comparison of the rate constants of k_2 and k_3 suggests that the overall reaction to form propynal is faster than the competing process to yield cyclopropenone by a factor of about 4. Also, the pre-exponential factors, which are indicative of geometrical constraints of the reactions, show that concentration of $[\text{CO}-\text{C}_2\text{H}_2]$ complexes in the correct geometrical orientation leading to propynal are higher by a factor of about 2 than those forming the cyclic isomer. This could be understood in terms of the cone of acceptance of the acetylene molecule. Here, the formation of cyclopropenone requires that carbon

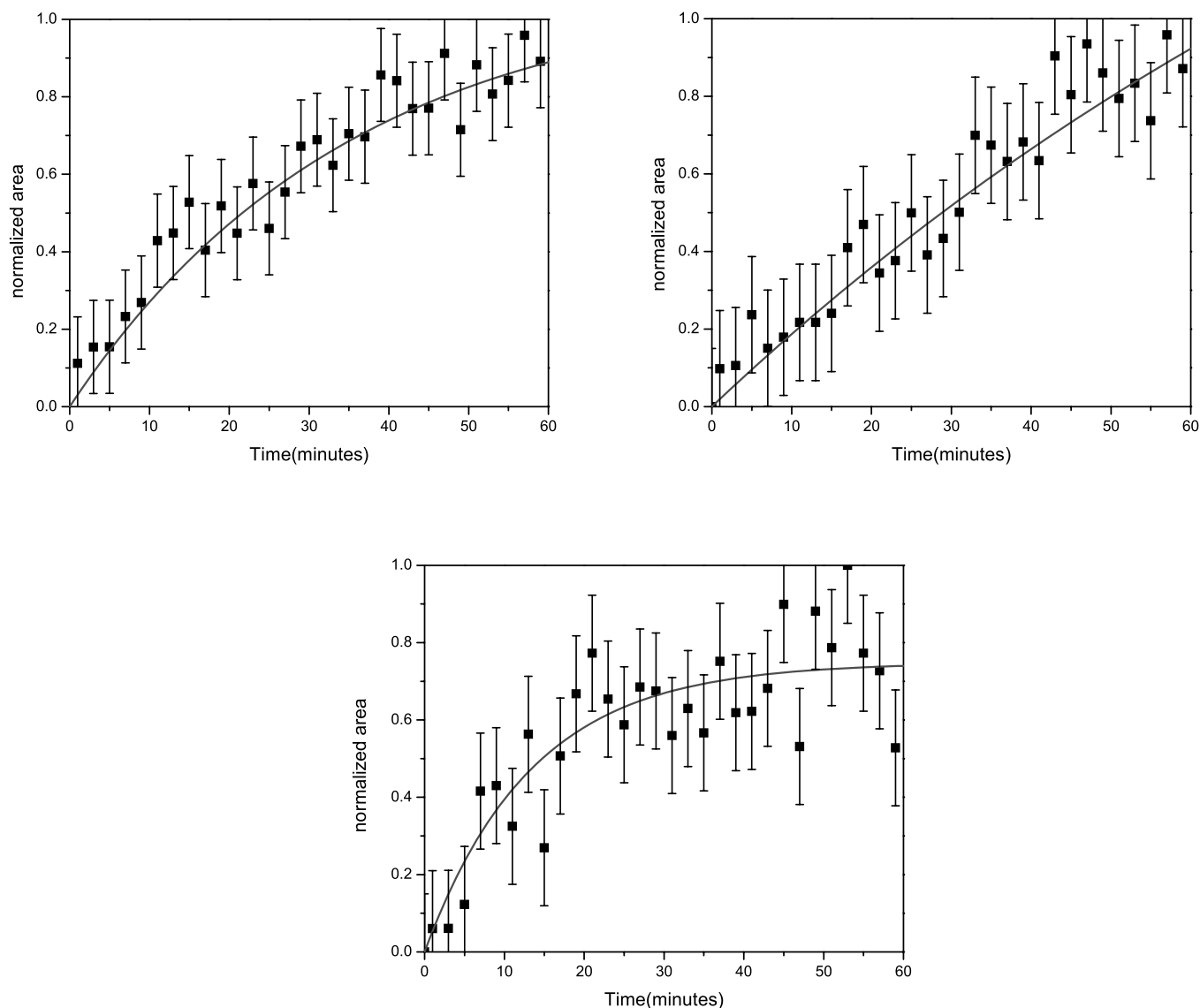


FIG. 4.—Temporal evolution of cyclopropenone (*top left*), propynal (*top right*), and the formyl radical (*bottom*). [See the electronic edition of the Journal for a color version of this figure.]

monoxide adds to the carbon-carbon triple bond. This requires a reaction geometry in the matrix where the carbon atom of the carbon monoxide molecule points toward the π -electronic system of the acetylene molecule. However, a radical-radical recombination reaction of the ethynyl with the formyl radical has less geometrical constraints, except that both radicals should be close enough so that radical centers can recombine,

$$[\text{HCO}](t) = a(1 - e^{-k_1 t}), \quad (10)$$

$$[\text{HCCCHO}](t) = b(1 - e^{-k_2 t}), \quad (11)$$

$$[\text{c-C}_3\text{H}_2\text{O}](t) = c(1 - e^{-k_3 t}). \quad (12)$$

To convert the integrated areas into column densities and absolute numbers of synthesized molecules, we utilized the integral absorption coefficients of the 1481 cm^{-1} ($A = 1.88 \times 10^{-18} \text{ cm}^{-1}$) and 1841 cm^{-1} ($A = 1.02 \times 10^{-16} \text{ cm}^{-1}$; cyclopropenone), 2112 cm^{-1} ($A = 1.55 \times 10^{-16} \text{ cm}^{-1}$) and 962 cm^{-1} ($A = 3.80 \times 10^{-18} \text{ cm}^{-1}$; propynal), and of 1845 cm^{-1} ($A = 1.50 \times 10^{-17} \text{ cm}^{-1}$; formyl; Bennett et al. 2005b). This leads

to column densities at the end of the irradiation phase of $(0.9 \pm 0.6) \times 10^{15} \text{ cm}^{-2}$ (cyclopropenone), $(0.8 \pm 0.6) \times 10^{15} \text{ cm}^{-2}$ (propynal), and $(0.3 \pm 0.1) \times 10^{15}$ (formyl); the total number of molecules computed to $(2.7 \pm 1.8) \times 10^{15}$ (cyclopropenone), $(2.4 \pm 1.8) \times 10^{15} \text{ cm}^{-2}$ (propynal), and $(0.9 \pm 0.3) \times 10^{15}$, i.e., a formation of about 1.5 ± 1.0 cyclopropenone, 1.5 ± 1.0 propynal, and 0.6 ± 0.2 formyl radicals per implanted electron. Considering the energy deposited into the system, we can compute average production rates of about $(4 \pm 2) \times 10^{-3}$ (cyclopropenone), $(4 \pm 2) \times 10^{-3}$ (propynal), and $(1.6 \pm 0.6) \times 10^{-3}$ (formyl) molecules per eV.

Finally, to confirm the derived reaction mechanisms theoretically, we conducted computations on the singlet and triplet $\text{C}_3\text{H}_2\text{O}$ potential energy surfaces (PES; Fig. 5). The computations show that on the singlet surface two addition pathways exist. These are the formation of cyclopropenone (s1) and an acyclic isomer (s2) by addition to two and one carbon atoms via barriers of 390 and 159 kJ mol^{-1} , respectively. Both structures are connected via ring opening/closure processes. The acyclic structure (s2) can isomerize via hydrogen shift to form propynal (s3) and propadienone (s4) via barriers of 160 and 195 kJ mol^{-1} ,

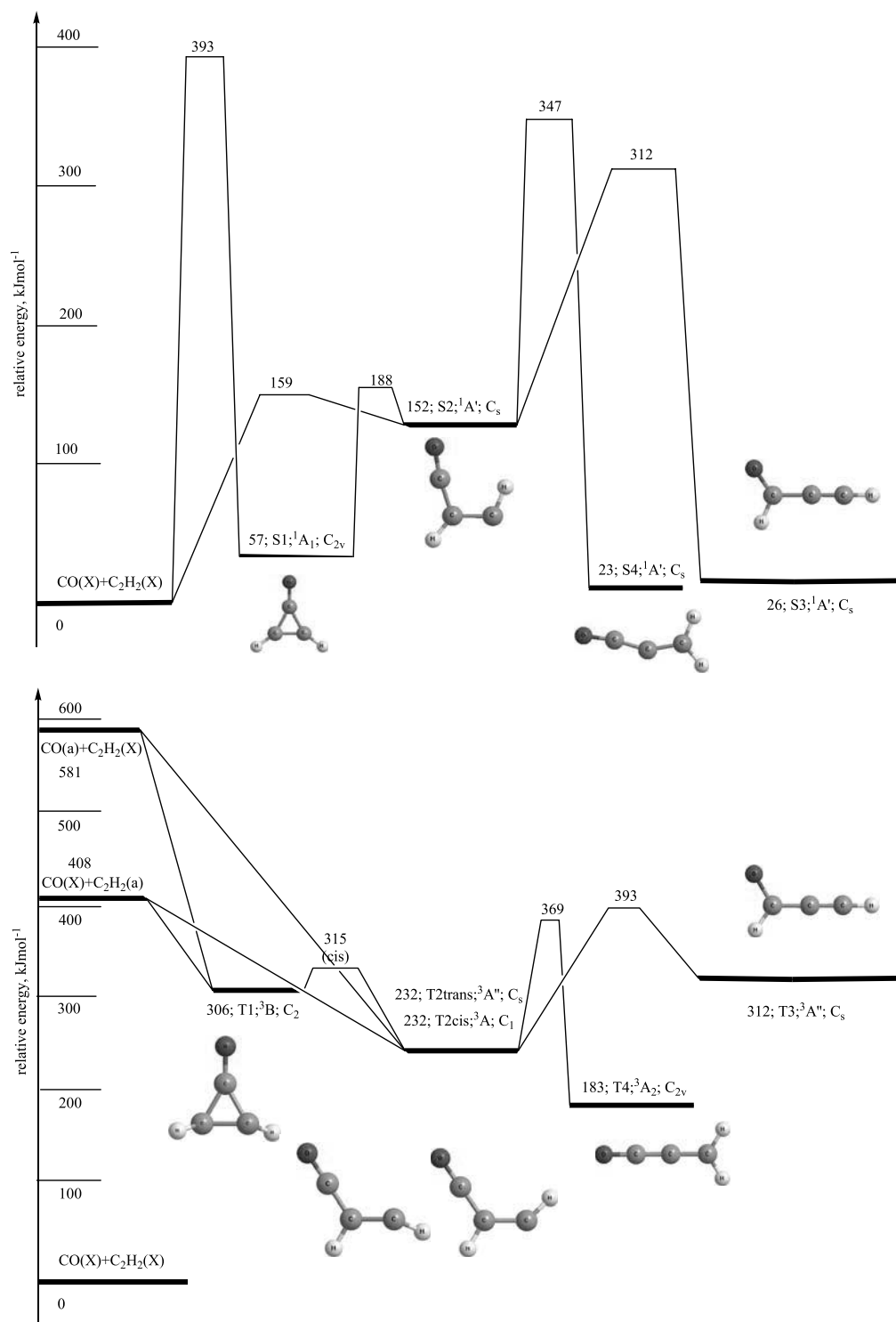


FIG. 5.— Singlet (*top*) and triplet (*bottom*) C_3H_2O potential energy surface relevant to the formation of cyclopropenone and propynal in extreme environments. Energies were computed at the CCSD(T)/cc-pVTZ level of energy and were corrected for zero-point energies. Point groups and electronic wave functions are also indicated. “X” indicates the electronic ground states, and “a” the first excited triplet states of the reactants.

respectively. Note that on the singlet surface, no one-step pathway exists to the form propynal (s3). On the triplet surface, two addition pathways have been located as well: the formation of triplet cyclopropenone (t1) and the acyclic isomer (t2). It should be stressed that intrinsic reaction coordinate calculations suggest that the reactions from $CO(a^3\Pi) + C_2H_2(X^1\Sigma_g^+)$ and $CO(X^1\Sigma^+) + C_2H_2(a^3A_u)$ to t1 and t2 are all barrier-less.

How can we combine the computations with the experimentally derived data to derive the actual reaction mechanism? Let us focus on the formation of cyclopropenone first. The kinetic profile derived from the infrared data proposed a (pseudo-) first order mechanism of a $CO-C_2H_2$ complex in the correct geometrical orientation. Our calculations suggest that due to the high barrier on the singlet surface, a one-step mechanism via addition

from the thermal ground state reactants on the singlet surface is not likely. However, the impinging electron can excite the carbon monoxide and/or the acetylene molecule to the first excited triplet state (Fig. 5) so that a barrier-less addition to t1 and t2 is feasible. In the matrix, t1 can undergo a rapid intersystem crossing to yield singlet cyclopropenone (s1). This scenario can account for the experimental data. Based on the calculations, the addition-isomerization pathway to propynal might be an alternative route to reactions (7)–(9). However, the experiments do not allow a distinct discrimination between both possibilities. Nevertheless, the experiments, energetics, and computations suggest that a formation of both cyclopropenone and propynal on electron irradiation in ices is feasible.

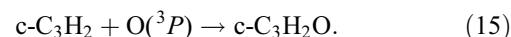
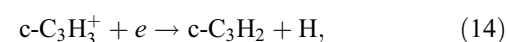
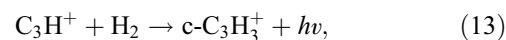
6. ASTROPHYSICAL IMPLICATIONS

Our laboratory experiments suggest that both the cyclopropenone and propynal molecules (Fig. 1) can be formed in electron irradiated carbon monoxide-acetylene ices at 10.4 K. Although carbon monoxide is a well-known constituent of ice-coated interstellar grains in cold molecular clouds (Fraser et al. 2002; Ehrenfreund & Schutte 2000; Gibb et al. 2004), the acetylene reactant has not been observed on ices so far. However, laboratory experiments indicated that a charged particle processing of methane ices (CH₄) at 10 K leads to a formation of complex hydrocarbon molecules, among them acetylene. Therefore, acetylene is predicted to exist on processed, interstellar grains at a level of less than 1% compared to water (H₂O; Kaiser & Roessler 1997; Bennett et al. 2006). Based on our studies, we can therefore predict that a processing of ice-coated, interstellar grains by Galactic cosmic ray particles, which in turn generate high-energy electrons within the ices, can lead to the synthesis of *both* cyclopropenone and propynal molecules in cold molecular clouds. Recall that the overall reactions to form cyclopropenone and propynal from the acetylene and carbon monoxide reactants are calculated to be *endoergic* by 30 and 10 kJ mol⁻¹, respectively. Therefore, thermal reactants cannot form these isomers in the low-temperature ices as present on interstellar grains; an external energy source such as energetic cosmic ray particles triggering secondary electrons is clearly required to compensate for the endoergicity of the reaction. These considerations underline the role of nonequilibrium (suprathermal) chemistry in the formation of organic molecules in extraterrestrial ices.

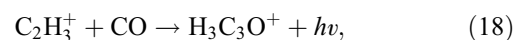
In star-forming regions such as Sgr B2, molecules synthesized on icy grains in the molecular cloud phase can be released into the gas phase by sublimation so that detection via microwave spectroscopy is feasible. Our proposed formation of cyclopropenone on icy grains is supported by a recent modeling study of Quan & Herbst (2007). Here, the authors concluded that a pure gas phase model cannot explain the observed fractional abundances of cyclopropenone as observed toward Sgr B2(N). Therefore, an incorporation of cosmic ray processed ices followed by sublimation might be a crucial aspect to account for the observed abundance of the cyclopropenone isomer in hot molecular cores. On the other hand, it is surprising that searches toward Sgr B2(N) failed to detect the propynal molecule. Various possibilities might account for this scenario. First, considering the derived column densities and the inherent error limits in our experiments of $(0.9 \pm 0.6) \times 10^{15}$ cm⁻² (cyclopropenone), $(0.8 \pm 0.6) \times 10^{15}$ cm⁻² (propynal), it should be noted that within the error limits, propynal might be 1 order of magnitude less abundant than cyclopropenone. Alternatively, the intense UV field from the newly formed stars in Sgr B2 might lead to a preferential photodestruction of the propynal isomer in the gas phase. However, gas phase photodissociation experiments of cycloprope-

none and propynal are absent so far. Finally, propynal might react preferentially—compared to cyclopropenone—in hot molecular cores. However, similar to missing photodissociation studies, reactions of these molecules with astrophysically relevant molecules in the gas phase have not been conducted so far.

We would like to stress that the formation of cyclopropenone on interstellar ices might also explain the hitherto failed detection in cold molecular clouds like TMC-1, where—due to the low temperature of 10 K—molecules formed on interstellar grains cannot sublime into the gas phase. The solid-state route also presents a strong alternative to hitherto postulated gas phase reactions leading to this molecule; recall that gas phase reactions (13)–(15) cannot reproduce the observed abundances in Sgr B2(N) (Quan & Herbst 2007),



On the other hand, propynal can be formed in the gas phase of, for example, cold molecular clouds, via barrier-less reactions of atomic oxygen with propargyl radicals (eq. [16]; Kwon et al. 2006), and also by bimolecular collisions of ethynyl radicals with formaldehyde (H₂CO) (eq. [17]; Petrie 1995). Alternative ion-molecule reactions (18)–(19) have been discussed as well (Irvine et al. 1988),



Summarized, our laboratory studies suggest that the formation of cyclopropenone (c-C₃H₂O) can be explained by a synthesis on interstellar, icy grains under nonequilibrium chemistry conditions in cold molecular clouds followed by a sublimation of the grains once the hot core stage is reached. Propynal can be synthesized on icy grains, too, but gas phase neutral-neutral and ion-molecule reactions can explain its observed abundances in cold clouds within the observational and modeling constraints as well. Future laboratory experiments will also investigate to what extent cyclopropenone can undergo an electron irradiation induced isomerization to propynal and vice versa.

7. SOLAR SYSTEM APPLICATIONS

Gas phase chemical processes in the atmospheres of solar planets and their satellites have been explored and well established for years (e.g., Strobel & Yung 1979; Yung et al. 1984; Yung & DeMore 1999; Moses et al. 2005; Strobel 2005). However, the solid state and aerosol chemistry has remained poorly explored, especially for Titan's atmosphere. Here, the hydrocarbon chemistry and aerosol formation rates are highly enhanced compared to other solar system objects. One of the limiting factors is the lack of experimental data which are fundamental for atmospheric chemical modeling. Here, we present a first attempt to model the formation of oxygen compounds via heterogeneous chemistry, utilizing the experimentally derived yields of chemical species produced from the irradiation of CO-C₂H₂ solid mixture

determined in this work. Titan is selected for detailed modeling study because of its rich chemistry and abundant observations.

Titan is Nature's laboratory for organic synthesis. Because of Titan's low gravity, which allows light species such as hydrogen to escape readily (e.g., Yelle et al. 2006), processes that recycle hydrocarbons back to CH₄ through the interaction of hydrogen are greatly reduced, resulting in higher abundance of hydrocarbons in the atmosphere of Titan and a hazy atmosphere by subsequent physiochemical processes that turn gaseous species into aerosols (e.g., Liang et al. 2007). A previous study suggests that pure gas phase photochemistry produces hydrocarbon abundances that are *too high* in the regions where most of hydrocarbons are synthesized (Liang et al. 2007). Mechanisms that physically adsorb molecules on existing aerosols followed by UV and/or cosmic-ray irradiation that convert adsorbed molecules permanently into tholins are proposed in order to reduce gaseous hydrocarbons and to explain the aerosol profiles above 350 km derived from *Cassini* UVIS observations (Liang et al. 2007). Here, we explore the cosmic-ray-induced processes on those aerosol particles and make a comparison with pure gas phase chemistry. For this study, we select Model D of Liang et al. (2007). The low-energy cosmic ray particles that are used to dissociate/ionize molecular nitrogen are not considered here, because those cosmic ray particles cannot reach the surface; in addition, the interaction cross sections between low-energy cosmic rays and atmospheric aerosols are too small to have a noticeable contribution to atmospheric chemical production. Therefore, we consider high-energy cosmic ray particles at the surface of Titan. The energy flux at the surface is estimated to be 10⁹ eV cm⁻² s⁻¹ (Sagan & Thompson 1984).

A model which incorporates the obtained radiation yields of C₃H₂O, c-C₃H₂O, and HCO from the experiments as described above is developed. The heterogeneous production of both C₃H₂O isomers was found to be orders of magnitude higher than the gaseous chemistry; in addition, heterogeneous chemistry is the only known source for c-C₃H₂O. The integrated production rates of C₃H₂O by gaseous and heterogeneous chemistries are 3 × 10⁴ and 5 × 10⁶ molecules cm⁻² s⁻¹, respectively. These

numbers alone clearly indicate that heterogeneous chemistry must not be neglected. Further, the production rate of c-C₃H₂O is determined to be 5 × 10⁶ molecules cm⁻² s⁻¹. The production of HCO by gaseous chemistry (2 × 10⁸ molecules cm⁻² s⁻¹) is 2 orders of magnitude higher than that by heterogeneous chemistry (2 × 10⁶ molecules cm⁻² s⁻¹). However, the atmospheric chemical processes play a small role at the surface, because HCO is close to being in photochemical equilibrium, resulting in negligible downward transport flux near the surface. The loss processes for C₃H₂O and c-C₃H₂O remain undetermined, so the vertical profiles of the abundances, which provide direct comparison to observations, of these two cannot be derived from the current model. Further laboratory measurements on the destruction pathways are needed. Note that in the above calculation, we have assumed that the heterogeneous productions of C₃H₂O and c-C₃H₂O are limited by the amount of C₂H₂ in the aerosol. The total meteoritic impact rate (a source of oxygen) is ~10⁻¹⁶ g cm⁻² s⁻¹ (Moses et al. 2005), which is close to the influx of oxygen (H₂O is assumed) of 1.5 × 10⁶ molecules cm⁻² s⁻¹ at the top of the atmosphere used in the current model (based on Yung et al. 1984), comparable to the amount of oxygen compounds produced by cosmic-ray irradiation. The amount of oxygen compounds in impacting particles preserved in the solid phase, which affects the heterogeneous production of oxygen compounds, is uncertain. Similar mechanisms also apply to terrestrial planets and icy satellites, such as Mars and Enceladus.

The experimental work was supported by the Chemistry division of the US National Science Foundation (NSF-CRC CHE-0627854). L. G. G. and A. H. H. C. wish to thank the National Center for High Performance Computer of Taiwan for the support of computer resources. M. C. L. was supported by an NSC grant to Academia Sinica and by grant NSC 97-2628-M-001-001. Y. L. Y. was supported by NASA grant NNX07AI63G to the California Institute of Technology.

REFERENCES

- Baines, K. H., et al. 2006, *Planet. Space Sci.*, 54, 1552
 Becke, A. D. 1993, *J. Chem. Phys.*, 98, 5648
 Beer, R. 1975, *ApJ*, 200, L167
 Bell, E. E., & Nielsen, H. H. 1950, *J. Chem. Phys.*, 18, 1382
 Bennett, C. J., Chen, S. H., Sun, B. J., Chang, A. H. H., & Kaiser, R. I. 2007, *ApJ*, 660, 1588
 Bennett, C. J., Jamieson, C. S., Mebel, A. M., & Kaiser, R. I. 2004, *Phys. Chem. Chem. Phys.*, 6, 735
 Bennett, C. J., Jamieson, C. S., Osamura, Y., & Kaiser, R. I. 2005a, *ApJ*, 624, 1097
 ———. 2006, *ApJ*, 653, 792
 Bennett, C. J., Osamura, Y., Lebar, M. D., & Kaiser, R. I. 2005b, *ApJ*, 634, 698
 Bernard, J.-M., Coll, P., Coustenis, A., & Raulin, F. 2003, *Planet. Space Sci.*, 51, 1003
 Bockelee-Morvan, D., Lellouch, E., Biver, N., Paubert, G., Bauer, J., Colom, P., & Lis, D. C. 2001, *A&A*, 377, 343
 Brown, F. R., Finseth, D. H., Miller, F. A., & Rhee, K. H. 1975, *J. Am. Chem. Soc.*, 97, 1011
 Chapman, O. L., Miller, M. D., & Pitzengerger, S. M. 1987, *J. Am. Chem. Soc.*, 109, 6867
 Courtin, R., Gautier, D., & Strobel, D. 1996, *Icarus*, 123, 37
 de Kok, R., et al. 2007, *Icarus*, 186, 354
 Drouin, D., Couture, A. R., Gauvin, R., Hovington, P., Horny, P., & Demers, H. 2001, *Monte Carlo Simulation of Electron Trajectory in Solids (CASINO)* (ver. 2.42; Sherbrooke: Univ. Sherbrooke)
 Dunning, T. H. 1989, *J. Chem. Phys.*, 90, 1007
 Ehrenfreund, P., & Schutte, W. A. 2000, in *IAU Symp. 197, Astrochemistry: From Molecular Clouds to Planetary Systems*, ed. Y. C. Minh & E. F. van Dishoeck (San Francisco: ASP), 135
 Forney, D., Jacox, M. E., & Thompson, W. E. 1995, *J. Mol. Spectrosc.*, 170, 178
 Fraser, H. J., McCoustra, M. R. S., & Williams, D. A. 2002, *Astron. Geophys.*, 43, 10
 Frisch, M. J., et al. 2001, *Gaussian 98* (Rev. A.9; Pittsburgh: Gaussian, Inc.)
 Gibb, E. L., Whittet, D. C. B., Boogert, A. C. A., & Tielens, A. G. G. M. 2004, *ApJS*, 151, 35
 Guzmán, R., Gallego, J., Koo, D. C., Phillips, A. C., Lowenthal, J. D., Faber, S. M., Illingworth, G. D., & Vogt, N. P. 1997, *ApJ*, 489, 559
 Hollis, J. M., Remijan, A. J., Jewell, P. R., & Lovas, F. J. 2006, *ApJ*, 642, 933
 Irvine, W. M., Brown, R. D., Cragg, D. M., Friberg, P., Godfrey, P. D., Kaifu, N., Matthews, H. E., Ohishi, M., Suzuki, H., & Takeo, H. 1988, *ApJ*, 335, L89
 Jamieson, C. S., Mebel, A. M., & Kaiser, R. I. 2006, *ApJS*, 163, 184
 Jiang, G. J., Person, W. B., & Brown, K. G. 1975a, *J. Chem. Phys.*, 43, 3734
 ———. 1975b, *J. Chem. Phys.*, 64, 1201
 Jursic, B. S. 1998, *J. Mol. Struct.*, 427, 157
 Kaiser, R. I. 2002, *Chem. Rev.*, 102, 1309
 Kaiser, R. I., & Roessler, K. 1997, *ApJ*, 475, 144
 Keller, H.-M., Floethmann, H., Dobbyn, A. J., Schinke, R., Werner, H.-J., Bauser, C., & Rosmus, P. 1996, *J. Chem. Phys.*, 105, 4983
 King, G. W., & Moule, D. 1961, *Spectrochim. Acta*, 17, 286
 Krishnan, R., Binkley, J. S., Seeger, R., & Pople, J. A. 1980, *J. Chem. Phys.*, 72, 650
 Kwon, L. K., Nam, M. J., Youn, S. E., Joo, S. K., Lee, H., & Choi, J. H. 2006, *J. Chem. Phys.*, 124, 204320
 Lee, C., Yang, W., & Parr, R. G. 1988, *Phys. Rev. B*, 37, 785
 Liang, M. C., Yung, Y. L., & Shemansky, D. E. 2007, *ApJ*, 661, L199
 McLean, A. D., & Chandler, G. S. 1980, *J. Chem. Phys.*, 72, 5639
 Moses, J. I., Fouchet, T., Bezaud, B., Gladstone, G. R., Lellouch, E., & Feuchtgruber, H. 2005, *J. Geophys. Res.*, 110, E08001

- Nakayama, T., & Watanabe, K. 1964, *J. Chem. Phys.*, 40, 558
- Noll, K. S., Knacke, R. F., Geballe, T. R., & Tokunaga, A. T. 1986, *ApJ*, 309, L91
- Nummelin, A., Dickens, J. E., Bergman, P., Hjalmarsen, Å., Irvine, W. M., Ikeda, M., & Ohishi, M. 1998, *A&A*, 337, 275
- Petrie, S. 1995, *ApJ*, 454, L165
- Purvis, G. D., & Bartlett, R. J. 1982, *J. Chem. Phys.*, 76, 1910
- Quan, D., & Herbst, E. 2007, *A&A*, 474, 521
- Raghavachari, K., Trucks, G. W., Pople, J. A., & Head-Gordon, M. 1989, *Chem. Phys. Lett.*, 157, 479
- Rosenqvist, J., Lellouch, E., Romani, P. N., Paubert, G., & Encrenaz, T. 1992, *ApJ*, 392, L99
- Sagan, C., & Thompson, W. R. 1984, *Icarus*, 59, 133
- Stephens, J. W., Yan, W.-B., Richnow, M. L., Solka, H., & Curl, R. F. 1988, *J. Mol. Struct.*, 190, 41
- Strobel, D. F. 2005, *Space Sci. Rev.*, 116, 155
- Strobel, D. F., & Yung, Y. L. 1979, *Icarus*, 37, 256
- Tarasova, O. A. 1982, *Zh. Organ. Khim.*, 18, 2042
- Tørneng, E., Nielsen, C. J., & Klaeboe, P. 1980, *Spectrochim. Acta*, 36A, 975
- Turner, B. E. 1991, *ApJS*, 76, 617
- Wang, H. Y., Eyre, J. A., & Dorfman, L. M. 1973, *J. Chem. Phys.*, 59, 5199
- Werner, H.-J., Bauer, C., Rosmus, P., Keller, H.-M., Stumpf, M., & Schinke, R. 1995, *J. Chem. Phys.*, 102, 3593
- Woon, D. E. 1996, *J. Chem. Phys.*, 105, 9921
- Yelle, R. V., Borggren, N., de la Haye, V., Kasprzak, W. T., Niemann, H. B., Muller-Wodarg, I., & Waite, J. H. 2006, *Icarus*, 182, 567
- Yung, Y. L., Allen, M., & Pinto, J. P. 1984, *ApJS*, 55, 465
- Yung, Y. L., & DeMore, W. D. 1999, *Photochemistry of Planetary Atmospheres* (New York: Oxford Univ. Press)